ac-Stark-effect-enhanced four-wave mixing in a near-resonant four-level system

Chen-Yu Tai, R. T. Deck, and Charles Kim
Department of Physics and Astronomy, University of Toledo, Toledo, Ohio 43606
(Received 29 December 1986)

We report on an ac-Stark-effect-enhanced wave-mixing experiment in I_2 vapor in which an output uv signal at frequency $2\omega_1+\omega_2$ is maximized when the input frequencies ω_1 and ω_2 are both detuned in the same direction from the resonance frequencies of the free molecule. A theory based on a configuration interaction between the "dressed molecular levels" is presented to explain the strong enhancement of the uv signal under these conditions. The data presented demonstrate that tunable coherent radiation at ultraviolet and vacuum-ultraviolet frequencies can be generated by the wave-mixing process we describe.

I. INTRODUCTION

The ac Stark effect[1-3] in two-level systems has been intensively studied[2-12] in the case of optical transitions. In a two-level system the ac Stark effect is studied by observing the optical Autler-Townes splitting[6,7] and radiative shift[8,9] in atoms in spontaneous emission and in absorption to a third level as well as in stimulated processes.[10,11] In this work it will be shown that the ac Stark effect in a four-level system can be studied by the observation of resonant enhancement in a situation in which neither the one-, two-, nor three-quantum transition is in resonance with the exciting beams.

ac-Stark-effect-enhanced wave mixing in a four-level system has recently been observed in I_2 vapor.[13,14] In the reported work, a strong laser beam, at frequency ω_1, was used to excite both the first two excited quantum states $|1\rangle$ and $|2\rangle$ in I_2 molecules as the result of an accidental coincidence in the one- and two-quantum transition frequencies $|0\rangle$-$|1\rangle$ and $|1\rangle$-$|2\rangle$.[15] A second and weaker beam, at frequency ω_2, was then used to probe the ac-Stark-shifted "dressed levels"[16] of the molecule–laser-field system by means of wave mixing through a fourth molecular level, $|3\rangle$. Configuration interaction among the excited dressed levels, $|1'\rangle$ and $|2'\rangle$, was studied by observation of intensity variations in the mixed-wave signal at frequency $2\omega_1+\omega_2$ along with correlations between the wavelengths of the two laser beams corresponding to mixed-wave resonances. The mixed-wave signal was observed to have its maximum intensity when the input frequencies ω_1 and ω_2 were both detuned in the *same* direction from the resonance frequencies of the free molecule. Since the resonance frequency in one input beam, ω_2, may be controlled by the frequency and intensity of the other beam, ω_1, this effect allows for the production of a large output signal at the high frequency, $2\omega_1+\omega_2$, over an appreciable range of ω_1 and ω_2 values.

In this work we present a large amount of additional experimental data on the enhanced wave mixing in the I_2 molecular system. We precede this in Sec. II by discussion of a semiclassical theory of the wave-mixing process that provides a physical picture of the mechanism responsible for the observed resonant enhancement which is not predicted by the usual approach to the theory. In particular, we explain the ac-Stark-effect-enhanced resonance in terms of a "beating" between the signals which oscillate with the four Rabi-shifted frequencies.

The experimental data presented in Sec. III confirm the fact reported earlier[13] that the uv signal at frequency $2\omega_1+\omega_2$ is maximized when both input frequencies are detuned in the *same* direction from the resonance frequencies in the free molecule. The data show in particular that when the wavelength $\lambda(1)$ of input beam 1 is increased, a maximum in the uv output signal is produced when the wavelength $\lambda(2)$ of input beam 2 is also increased. In addition, the data presented in Sec. III show that in a graph of the $\lambda(2)$ versus $\lambda(1)$ values corresponding to a local maximum in the output signal, a discontinuity occurs in the graph at a value of the wavelength $\lambda(1)$ close to the value of $\lambda(1)$ for which the uv signal is maximized. Because this discontinuity is found to increase with the input power of beam 1, it can be inferred to be a consequence of the ac Stark effect. We conclude Sec. III with a comparison between the experimental results and the theoretical predictions derived from Sec. II.

II. THEORY

The standard theory of wave mixing[17] (which involves diagrammatic techniques) is based on perturbation theory with the matrix elements of the interaction potential, $H_{\rm int}$, taken to be perturbation parameters. Because in the case studied here the intensity of the input laser beam at frequency ω_1 needs in practice to be quite large to allow for an appreciable signal in the mixed wave, this perturbative approach is not valid, and we need therefore to adopt a nonperturbative approach. The usual method for calculating observables in a two-level system under this circumstance is to begin with the optical Bloch equations. In the case of a four-level system, however, this approach becomes untractable and instead we choose a different method of analysis in which we solve the time-dependent equation for the density matrix in an

interaction picture. This method of analysis allows us to develop a physical picture of the ac Stark effect enhancement in the output intensity.

Two other nonperturbative approaches[18,19] to the analysis of the interaction between radiation and multilevel systems should be cited. The first[18] develops the theory of a three-level system in interaction with two near-resonant laser fields under the assumption of a steady-state condition, while the second[19] considers the more general case of an n-level system in interaction with $n-1$ near-resonant fields and presents the results of a numerical solution of the Schrödinger equation for the time dependence of the level populations. Reference 18 focuses on the spectra of the absorbed and elastically scattered radiation rather than on the spectrum of the radiation scattered in a coherent process of wave mixing, which is the focus of the present work. It is shown in Ref. 18, under the condition that the dipole matrix elements connecting distinct pairs of levels are unequal, that a resonance can occur in the absorption spectrum when the overall detuning is nonzero. This result is similar but not equivalent to a result we discuss here.

The energy-level diagram for the four-level system with which we model the internal degrees of freedom of the I_2 molecule is shown in Fig. 1(a), with the ground-state level denoted $|0\rangle$. Transitions between the levels $|0\rangle$-$|1\rangle$, $|1\rangle$-$|2\rangle$, $|2\rangle$-$|3\rangle$, and $|3\rangle$-$|0\rangle$ are all assumed to be dipole allowed. Because the frequency spacing between the levels $|0\rangle$ and $|1\rangle$, and $|1\rangle$ and $|2\rangle$, is nearly equal in the I_2 molecule, it is possible with two incident laser frequencies to achieve near resonance in three allowed transitions.[13,15] In the experiment which we analyze here, an intense laser beam 1 at frequency ω_1 is tuned to be in near resonance with the transitions $|0\rangle$-$|1\rangle$ and $|1\rangle$-$|2\rangle$ simultaneously, while a weaker beam 2 at frequency ω_2 is tuned to be in near resonance with the transition $|2\rangle$-$|3\rangle$. Maxima in the output mixed-wave signal at frequency $2\omega_1+\omega_2$ are obtained by fixing the frequency ω_1 and scanning the frequency ω_2 until a maximum signal is recorded. Figures 1(b) and 1(c) show sets of energy levels of the combined system of molecule and laser field in the absence and in the presence of interaction between the molecule and field, respectively.

For the case of the intense laser field which we consider, it is sufficient to adopt a semiclassical description of the molecule-field interaction in which the field is described in terms of its classical electric field vector $\mathbf{E}(\mathbf{r},t)$. The total electric field vector associated with the incident laser beams at position $\mathbf{r}$ and time t can then be represented by the sum

$$\mathbf{E}(\mathbf{r},t)=\mathbf{E}_1(\mathbf{r},t)+\mathbf{E}_2(\mathbf{r},t)\ , \tag{1}$$

where

$$\mathbf{E}_i(\mathbf{r},t)=\mathcal{E}_i(\mathbf{r},t)\exp(-i\omega_i t+\mathbf{k}_i\cdot\mathbf{r})+\text{c.c.},\quad i=1,2 \tag{2}$$

and ω_i and $\mathbf{k}_i$ represent the frequency and wave vector of the ith field. We assume that the amplitude function $\mathcal{E}_i(\mathbf{r},t)$ in (2) is a slowly varying function of time which changes only slightly in the time interval $1/\omega_i$ and for

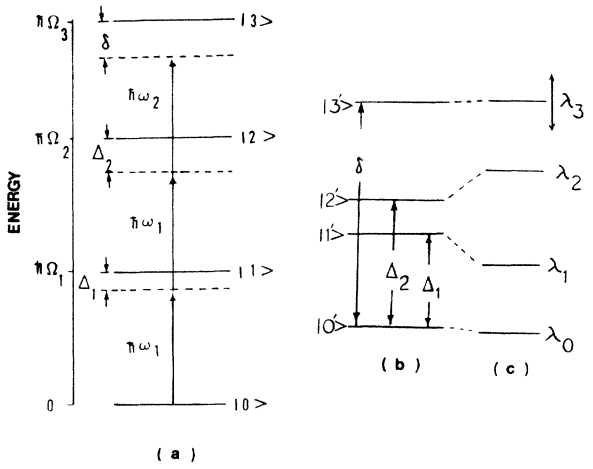

FIG. 1. Energy-level diagram for the system. (a) Energy levels of the free molecule shown in relation to laser photon energies. (Size of the detunings Δ_1, Δ_2, and δ is greatly exaggerated in this diagram.) (b) Particular set of energy levels of the total system of molecule and laser field in the absence of interaction. (c) Energy levels of the total system in the presence of interaction.

simplicity we take the electric field to be linearly polarized in the x direction. (The beams used in the experiment are circularly polarized but this makes no fundamental difference in the theory.) Since the generated wave is much weaker than the input beams, the field of the output radiation can be neglected in the total electric field.

The Hamiltonian that governs the evolution of the internal state of the molecule in the presence of the laser field can be written in the form

$$H=H_0+V\ , \tag{3}$$

where H_0 is the Hamiltonian for the unperturbed molecule and V is the molecule-field interaction potential defined by

$$V=-\boldsymbol{\mu}\cdot\mathbf{E}\ , \tag{4}$$

with $\boldsymbol{\mu}$ the dipole moment operator. The time evolution of the molecule's wave function is determined by H via the Schrödinger equation

$$i\hbar\frac{d}{dt}|\psi(t)\rangle=H|\psi(t)\rangle=(H_0+V)|\psi(t)\rangle\ . \tag{5}$$

We seek to make a transformation which simplifies the time dependence on the right-hand side of this equation. For this purpose we define a transformed ket $|\psi'(t)\rangle$ by the relation

$$|\psi'(t)\rangle=e^{iAt}|\psi(t)\rangle \tag{6}$$

and introduce a complete set of basis kets $|j\rangle$ defined by the eigenkets of H_0,

$$H_0|j\rangle=\hbar\Omega_j|j\rangle\ . \tag{7}$$

Then $|\psi'(t)\rangle$ satisfies the equation

$$i\hbar\frac{d}{dt}|\psi'(t)\rangle = H_\omega|\psi'(t)\rangle \ , \tag{8}$$

where

$$H_\omega = e^{iAt}(H_0+V-\hbar A)e^{-iAt} \ . \tag{9}$$

By choice of the operator A such that its matrix representation in the $|j\rangle$ basis has the form

$$A=\begin{bmatrix} 0 & 0 & 0 & 0 \\ 0 & \omega_1 & 0 & 0 \\ 0 & 0 & \omega_2 & 0 \\ 0 & 0 & 0 & 2\omega_1+\omega_2 \end{bmatrix}$$

and by use of the rotating-wave approximation to eliminate rapidly oscillating anti-resonance terms, the Hamiltonian H_ω can be reduced to a form that has no explicit dependence on time, which then allows Eq. (8) to be solved in the simple form,

$$|\psi'(t)\rangle = e^{-(i/\hbar)H_\omega t}|\psi'(0)\rangle \equiv M|\psi'(0)\rangle \ . \tag{10}$$

In particular, using the above representation for A we obtain H_ω in the form

$$H_\omega=\hbar\begin{bmatrix} 0 & a^* & 0 & 0 \\ a & \Delta_1 & b^* & 0 \\ 0 & b & \Delta_2 & c^* \\ 0 & 0 & c & \delta \end{bmatrix} \ . \tag{11}$$

Here Δ_1, Δ_2, and δ represent the detunings between the input frequencies and the resonance frequencies of the free molecule,

$$\begin{aligned} \Delta_1 &= \Omega_{10}-\omega_1 \ , \\ \Delta_2 &= \Omega_{20}-2\omega_1 \ , \\ \delta &= \Omega_{30}-2\omega_1-\omega_2 \ , \end{aligned} \tag{12}$$

and a,b,c denote dipole matrix element factors given by

$$a=-\mu_{10}\mathcal{E}_1\exp(i\mathbf{k}_1\cdot\mathbf{r}) \ ,$$

$$b=-\mu_{21}\mathcal{E}_1\exp(i\mathbf{k}_1\cdot\mathbf{r}) \ ,$$

and

$$c=-\mu_{32}\mathcal{E}_2\exp(i\mathbf{k}_2\cdot\mathbf{r}) \ .$$

These latter quantities carry all the information pertaining to the relative phase of the electric dipole moment of the molecule.

Given that H_ω can be represented in a form which has no explicit t dependence, Eq. (10) can be used to evaluate the time dependence of the molecular wave function. We first define a matrix S which diagonalizes the matrix representation of H_ω in the $|j\rangle$ basis according to the equation

$$SH_\omega S^{-1}=\lambda \ , \tag{13}$$

where λ is a diagonal matrix. After multiplication on the left by S^{-1}, the operator form of Eq. (13) can be written as

$$H_\omega S^{-1}=S^{-1}\lambda \ . \tag{14}$$

Multiplying on the right by the ket $|j\rangle$ and using the completeness relation $\sum_l |l\rangle\langle l|=1$, the last equation assumes the form

$$\begin{aligned} H_\omega S^{-1}|j\rangle &= S^{-1}\lambda|j\rangle \\ &= \sum_l S^{-1}|l\rangle\langle l|\lambda|j\rangle = \lambda_j S^{-1}|j\rangle \ , \end{aligned} \tag{15}$$

which demonstrates that the ket $S^{-1}|j\rangle$ is an eigenket of the operator H_ω associated with the eigenvalue λ_j. Since the matrix representations of the operators H_ω and λ need to be Hermitian, Eq. (13) requires that the matrix S have the property $S^\dagger=S^{-1}$, and the elements of the matrix representation of the jth eigenket of H_ω are therefore given by the complex conjugates of the elements in the jth row of the matrix representation of S, i.e.,

$$\langle n|S^{-1}|j\rangle = \langle j|S|n\rangle^* \ . \tag{16}$$

In what follows we will denote the eigenkets of the Hamiltonian H_ω by $|j'\rangle, j=0,1,2,3$. These kets and corresponding eigenvalues λ_j define the dressed levels of the molecule-field system. The matrix elements of S^{-1} then correspond to the expansion coefficients in the expansion of the dressed eigenkets in terms of the eigenkets of H_0. In particular,

$$|j'\rangle = S^{-1}|j\rangle = \sum_k (S^{-1})_{kj}|k\rangle = \sum_k S^*_{jk}|k\rangle \ . \tag{17}$$

In addition, since

$$\begin{aligned} \langle i|S^{-1}S|j\rangle &= \sum_k \langle i|S^{-1}|k\rangle\langle k|S|j\rangle \\ &= \sum_k S^*_{ki}S_{kj}=\delta_{ij} \ , \end{aligned}$$

the matrix elements of S satisfy the relation

$$\sum_k S^*_{ki}S_{kj}=\delta_{ij} \ . \tag{18}$$

Equation (13) allows the operator M of Eq. (10) to be expressed in the form

$$\begin{aligned} M=e^{-(i/\hbar)H_\omega t} &= S^{-1}Se^{-(i/\hbar)H_\omega t}S^{-1}S \\ &= S^{-1}e^{-(i/\hbar)SH_\omega S^{-1}t}S \\ &= S^{-1}e^{-(i/\hbar)\lambda t}S \end{aligned} \tag{19}$$

and it follows that

$$M^\dagger = S^\dagger e^{(i/\hbar)\lambda t}(S^{-1})^\dagger = S^{-1}e^{(i/\hbar)\lambda t}S = M^{-1} \ . \tag{20}$$

Because the matrix representation of λ is diagonal, the matrix representations of M and M^{-1} reduce to the forms

$$M_{jk}=\langle j \mid M \mid k \rangle$$
$$=\sum_{l,n}\langle j \mid S^{-1} \mid l \rangle\langle l \mid e^{-i(\lambda/\hbar)t} \mid n \rangle\langle n \mid S \mid k \rangle$$
$$=\sum_{l}(S^{-1})_{jl}(S)_{lk}e^{-i(\lambda_l/\hbar)t},$$
$$(M^{-1})_{jk}=\sum_{l}(S^{-1})_{jl}(S)_{lk}e^{i(\lambda_l/\hbar)t}. \tag{21}$$

By use of Eq. (6), the density operator $\rho(t)$ defined by the equation

$$\rho(t)=\mid \psi(t)\rangle\langle\psi(t) \mid \tag{22}$$

can be written in the form

$$\rho(t)=e^{-iAt} \mid \psi'(t)\rangle\langle\psi'(t) \mid e^{+iAt}$$
$$=e^{-iAt}\rho'(t)e^{+iAt}, \tag{23}$$

where, with the help of Eq. (10),

$$\rho'(t)=\mid \psi'(t)\rangle\langle\psi'(t) \mid =M \mid \psi'(0)\rangle\langle\psi'(0) \mid M^{-1}. \tag{24}$$

Since $\mid \psi'(0)\rangle=\mid \psi(0)\rangle$, the quantity $\mid \psi'(0)\rangle\langle\psi'(0) \mid$ can be identified with $\rho(0)$, and making use of Eq. (19), $\rho'(t)$ can be written as

$$\rho'(t)=S^{-1}e^{-(i/\hbar)\lambda t}S\rho(0)S^{-1}e^{(i/\hbar)\lambda t}S. \tag{25}$$

In the special case of interest where the matrix representation of $\rho(0)$ has the simple form

$$\rho_{jk}(0)=\delta_{j0}\delta_{k0}, \tag{26}$$

the matrix elements of $\rho'(t)$ reduce to

$$\rho'_{jk}(t)=M_{j0}(M^{-1})_{0k}=\left[\sum_{l}(S^{-1})_{jl}S_{l0}e^{-(i/\hbar)\lambda_l t}\right]$$
$$\times\left[\sum_{n}(S^{-1})_{0n}S_{nk}e^{i(\lambda_n/\hbar)t}\right]. \tag{27}$$

The matrix elements of the density operator $\rho(t)$ are then determined by Eq. (23). These latter matrix elements allow the expectation value of the dipole moment $\mathbf{P}$ of the molecule at position $\mathbf{r}$ and time t to be obtained by use of the equation

$$\langle \mathbf{P}(\mathbf{r},t)\rangle=\mathrm{Tr}[\mu\rho(\mathbf{r},t)]=\sum_{j,k}\mu_{kj}\rho_{jk}(\mathbf{r},t). \tag{28}$$

We are interested in the terms in the summation in Eq. (28) which contribute to the mixed-wave signal at the frequency $2\omega_1+\omega_2$. By use of Eq. (23) these terms can be expressed in the form

$$\mu_{03}\rho'_{30}(\mathbf{r},t)e^{-i(2\omega_1+\omega_2)t}+\text{c.c.}$$

Under conditions where a steady-state condition develops, the amplitudes $\rho'_{30}(\mathbf{r},t)$ of these terms averaged over the molecules in any volume element can be expected to be effectively time independent. Here we argue that molecular dephasing processes prevent the buildup of a macroscopic polarization and a judicious treatment of the time dependence of the amplitude ρ'_{30} is crucial for an interpretation of the observed signal. More specifically, we emphasize that the time evolution of the dipole moment of a given molecule can be assumed to follow from the equations of motion given above only during a time interval which is sufficiently short such that the molecule's distance of travel is appreciably less than the wavelength of the incident fields. For longer times the random motions of the molecules destroy the phase coherence of the field-induced dipole moments in the molecules in any volume element and the radiated coherent signal is suppressed. A strict treatment of this problem with homogeneous as well as inhomogeneous linewidth included is very complicated and will not be given in this paper. Instead we make use of Eq. (27) to explain the observed resonances in the wave-mixing process on the basis of level crossings between the dressed levels of the molecule-field system.

We first use Eqs. (27) and (16) to express the amplitude $\rho'_{30}(\mathbf{r},t)$ in the form

$$\rho'_{30}(\mathbf{r},t)=\left[\sum_{l}S^{*}_{l3}S_{l0}e^{-(i/\hbar)\lambda_l t}\right]\left[\sum_{n}S^{*}_{n0}S_{n0}e^{(i/\hbar)\lambda_n t}\right]. \tag{29}$$

Because we restrict use of the above form to short-time intervals such that $e^{(i/\hbar)\lambda_n t}$ is close to unity, Eq. (18) can be used to approximate the second factor in Eq. (29) by unity and the equation can be reduced to the result

$$\rho'_{30}(\mathbf{r},t)=\sum_{l}S^{*}_{l3}S_{l0}e^{-(i/\hbar)\lambda_l t}. \tag{30}$$

The required matrix elements of S in Eq. (30) can be determined by solution of Eq. (14) [and use of Eq. (16)]. In the case that the absolute values of the dipole matrix elements a, b, and c are small compared to the detunings Δ_1, Δ_2, and δ, the products $S^{*}_{l3}S_{l0}$ in the four separate terms in Eq. (30) can be approximated as follows:

$$(S^{*}_{03}S_{00})\cong\frac{abc}{\Delta_1\Delta_2\delta}, \tag{31a}$$

$$(S^{*}_{13}S_{10})\cong\frac{abc}{\Delta_1\Delta_2(\Delta_1-\delta)}, \tag{31b}$$

$$(S^{*}_{23}S_{20})\cong\frac{abc}{\Delta_1\Delta_2(\Delta_2-\delta)}, \tag{31c}$$

$$(S^{*}_{33}S_{30})\cong\frac{abc}{\delta(\Delta_1-\delta)(\Delta_2-\delta)}. \tag{31d}$$

On the basis of the above expressions it is possible to estimate the values of the overall detuning δ which should correspond to large mixed-wave signals at frequency $2\omega_1+\omega_2$. In particular, on the basis of Eqs. (31), resonant mixed-wave signals can be expected to occur at the δ values: $\delta=0$, Δ_1, and Δ_2. Figure 1(b) indicates that these δ values correspond to a crossing (or anticrossing) of level $\mid 3'\rangle$ with levels $\mid 0'\rangle$, $\mid 1'\rangle$, or $\mid 2'\rangle$. Whenever δ is close to one of the resonance values, two of the four terms in the sum in Eq. (30) are resonantly enhanced and can be assumed to dominate the remaining terms. Moreover, since the term proportional to $S^{*}_{33}S_{30}$ involves the product $\delta(\Delta_1-\delta)(\Delta_2-\delta)$ in its denominator, one of

the resonantly enhanced terms is always this term. Because the quantities $S^*_{k3}S_{k0}$ for all k must sum to zero by Eq. (18), the two dominant terms must be of equal amplitude but opposite sign, and the value of the sum in Eq. (30) for $t\neq 0$ must therefore derive from the beating between two terms of comparable amplitude but differing phase factors $e^{(i/\hbar)\lambda_l t}$.

It follows from the above that Eq. (30) can be simplified by approximating its right-hand side as the sum of two resonant terms in the form

$$\rho'_{30}\simeq S^*_{33}S_{30}e^{-(i/\hbar)\lambda_3 t}+S^*_{l3}S_{l0}e^{-(i/\hbar)\lambda_l t}$$
$$\cong S^*_{33}S_{30}e^{-(i/\hbar)\lambda_3 t}(1-e^{-(i/\hbar)(\lambda_l-\lambda_3)t}),$$
$$l=0,1,2\ . \tag{32}$$

For small time t (less than or equal to the effective coherent lifetime T), the above can be further reduced to the form

$$\rho'_{30}\cong(i/\hbar)(\lambda_l-\lambda_3)tS^*_{33}S_{30}\ . \tag{33}$$

In our experiment, where the strength of the interaction between the molecule and the field is significant, the dipole matrix elements a, b, and c may not be much smaller than Δ_1, Δ_2, and δ. In this case it is the dressed levels of Fig. 1(c) which are relevant rather than the interaction-free levels of Fig. 1(b), and the resonances in the mixed-wave signal as a function of δ can be expected to occur when the dressed level corresponding to the eigenvalue λ_3 crosses or anticrosses with a dressed level corresponding to the eigenvalue λ_0, λ_1, or λ_2. The latter three eigenvalues are determined by the strength and frequency of the strong laser beam at frequency ω_1 while the eigenvalue λ_3 is mainly determined by the frequency of the weak laser beam at frequency ω_2. Therefore, by fixing the frequency ω_1 and the resulting eigenvalues λ_0, λ_1, and λ_2 and measuring the mixed-wave signal as a function of the frequency ω_2, we are able to probe the eigenvalues of the dressed levels 0′, 1′, 2′ by monitoring the resonances in the mixed-wave signal corresponding to crossings (or anticrossings) of these levels with level 3′.

To illustrate the dependence of the eigenvalues λ_l on the frequency of the intense laser beam 1 we show in Fig. 2 a graph of the Stark shift of the dressed level 2 versus the value of Δ_2 for a fixed value of Δ_1 (taken to be equal to -20 GHz). The graph is constructed by solution of the eigenvalue equation (14) as a function of the parameter Δ_2 with the value of c set to zero. Inspection of the graph shows that the magnitude of the Stark shift of level 2 becomes a maximum ($\simeq 5$ GHz$\cong b/\hbar$) when the value of Δ_2 is equal to Δ_1, and, moreover, that the sign of the Stark shift reverses when the quantity $\Delta_2-\Delta_1$ changes from a positive to a negative value. A similar graph constructed for the Stark shift of dressed level 1 shows this shift to be of roughly equal magnitude but opposite sign to that of level 2. It follows that when ω_1 is varied such that $\Delta_2-\Delta_1$ changes sign, an abrupt change occurs in the positions of the dressed levels 1 and 2. In Sec. III we indicate that this change is reflected in

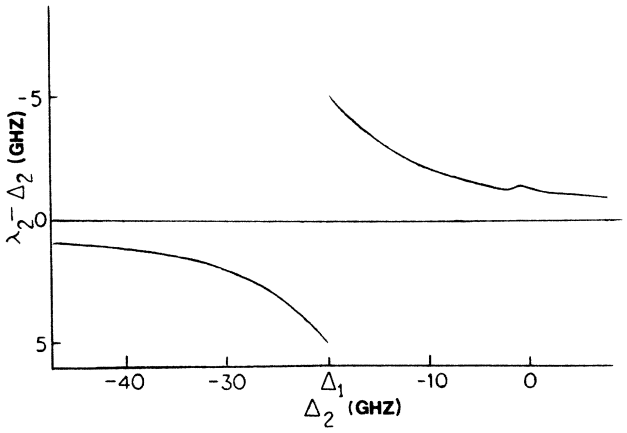

FIG. 2. ac Stark shift of the dressed level $|2'\rangle$ plotted as a function of the detuning Δ_2 of this level with a fixed detuning of the first level (-20 GHz) and the values of a and b set equal to 1 and 5 GHz, respectively. The magnitude of the Stark shift of level $|2'\rangle$ becomes a maximum ($\cong 5$ GHz) when the value of Δ_2 is equal to Δ_1, and the sign of the Stark shift reverses when the quantity $\Delta_2-\Delta_1$ changes from a positive to a negative value.

the observed spectrum of the mixed-wave signal as a discontinuity in the relationship between the wavelengths of the input laser beams which correspond to resonance maxima in the signal. This effect is a consequence of the fact that the resonances produced by the crossings of the level $|3'\rangle$ with the levels $|0'\rangle$, $|1'\rangle$, and $|2'\rangle$ are not all of equal intensity. This can be understood by way of the following argument. Equation (33) indicates that of the possible resonances which occur when the eigenvalue λ_3 is Stark shifted close to one of the eigenvalues λ_l, $l=0,1,2$, the dominant resonance corresponds to that for which the difference $\lambda_3-\lambda_l$ has the largest value. But the value of this difference can be established on the basis of the theory of nearly degenerate energy levels. In particular, the theory indicates that two nearly degenerate energy levels i and j, connected by a transition matrix element V_{ij}, must have eigenvalues which differ at their closest approach by $2|V_{ij}|$. In the case of the molecular energy levels considered in the present model, the level 3 is directly connected only to the levels 2 and 0, and (because of the weakness of the field at frequency $2\omega_1+\omega_2$) only the matrix element connecting the levels 3 and 2 is large ($\cong c$). Therefore, the eigenvalue difference $(\lambda_3-\lambda_2)$ associated with the resonance at $\delta\cong\lambda_2\cong\Delta_2$ can be expected to be larger than the eigenvalue differences associated with the other resonance values of δ.

On the basis of the above discussion and as a consequence of the fact that the dressed levels 2′ and 1′ interchange their positions when the sign of $\Delta_2-\Delta_1$ reverses, it can be expected that if the dominant resonance in the output signal is produced by the crossing of level 3′ with level 2′, in an experiment which determines the value of the wavelength $\lambda(2)$ of beam 2 which maximizes the output signal for a fixed value of the wavelength $\lambda(1)$ of

beam 1, the data will show a discontinuity in the resulting graph of the resonance values of $\lambda(2)$ versus $\lambda(1)$ in the vicinity of the $\lambda(1)$ value for which $\Delta_1=\Delta_2$. Since the condition $\Delta_1=\Delta_2$ in fact allows for a double resonance (level 2′ anticrosses level 1′ with $\Delta_2\cong\Delta_1$, and level 3′ anticrosses 2′ with $\delta\cong\lambda_2$), one can expect the maximum output signal to occur under this condition.

III. EXPERIMENT

The experimental setup for this work was described before.[13] Two laser beams of tunable frequencies ω_1 and ω_2 are combined colinearly by means of a Glan prism and focused to a cross section of approximately 0.1 mm^2 at the center of a 1-cm-long cell containing pure I_2 vapor at room temperature (vapor pressure $\sim$0.3 torr). The first laser (ω_1), produced by a Molectron DL-II dye laser pumped by a Molectron MY-32 Nd:YAG (neodymium-doped yttrium aluminum garnet) laser (10-nsec pulses), has a bandwidth and power of approximately 0.1 Å and 1.5 mJ/pulse, respectively, and is used to induce a two-photon excitation of the $|0\rangle$-$|2\rangle$ transition in the I_2 molecule. The second laser (ω_2) is provided by a National Research Group DL-3 dye laser pumped by the same Nd:YAG laser and has a bandwidth (at half-maximum) and power of approximately 0.4 Å and 40 μJ/pulse respectively. To eliminate production of background third-harmonic radiation by either laser, the two laser beams are converted to oppositely circularly polarized beams by means of a quarter-wave plate placed in front of the vapor cell. The mixed-wave signal produced by the two lasers at frequency $2\omega_1+\omega_2$ is separated from the laser beams by a prism, filtered by two narrow-band uv interference filters, and detected by a uv sensitive tube (EMI G-26G-315). The output signal is averaged by a boxcar integrator and displayed on a chart recorder.

With the second laser off, and the quarter-wave plate eliminated, the first beam is initially tuned to produce a maximum in the output signal at the third-harmonic frequency. This maximum is found to occur at a wavelength $\lambda(1)$ for beam 1 of 5629.2 Å, and is assumed to be produced at this wavelength by the occurrence of simultaneous resonances in the $|0\rangle$-$|1\rangle$ and $|1\rangle$-$|2\rangle$ transitions in the I_2 molecule.[13,15] The two laser beams are then mixed in the I_2 cell to produce an output uv signal at frequency $2\omega_1+\omega_2$.

Figure 3 shows observed spectra of the mixed-wave signal as a function of the wavelength $\lambda(2)$ of beam 2 for fixed values of $\lambda(1)$. Because the value of $\lambda(1)$ determines the two-photon transition which selects a particular second excited vibrational-rotational state of the molecule, the spectra of Fig. 3 can be interpreted to reflect the vibrational and rotational structure of the third excited quantum state of the I_2 molecule. Figure 3(a) shows the spectrum of the mixed-wave output when the wavelength of beam 2 is scanned from 5650 to 5900 Å with the wavelength $\lambda(1)$ of beam 1 fixed at the "double-resonance" value of 5629.2 Å. As expected, strong resonances in the mixed wave are observed when

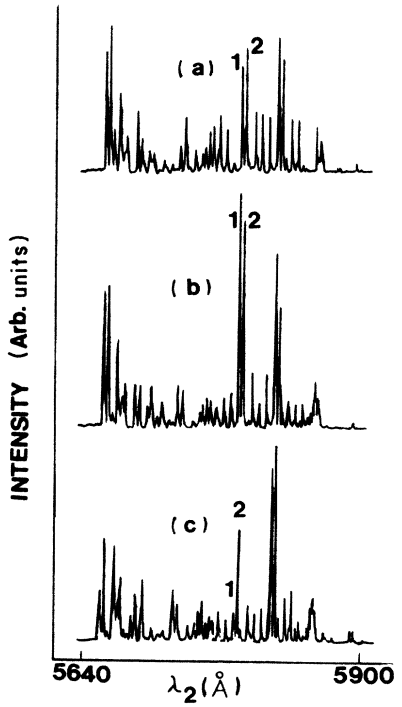

FIG. 3. Observed spectrum of mixed-wave signal as a function of the wavelength $\lambda(2)$ of beam 2 plotted for three distinct values of $\lambda(1)$: (a) $\lambda(1)=5629.2$ Å, (b) $\lambda(1)=5629.1$ Å, (c) $\lambda(1)=5627.7$ Å. Although the $\lambda(1)$ value in the graph in (a) represents the wavelength for beam 1 corresponding to a maximum in the third-harmonic signal, larger enhancements in the mixed-wave signal occur for the detuned values of $\lambda(1)$ corresponding to the graphs in (b) and (c).

$\lambda(1)$ is fixed at this value and the value of $\lambda(2)$ corresponds to a resonance in the $|2\rangle$-$|3\rangle$ transition.

Surprisingly, however, as shown in Figs. 3(b) and 3(c), when $\lambda(1)$ is fixed at the detuned values 5629.1 Å [in Fig. 3(b)] and 5627.7 Å [in Fig. 3(c)], variation of $\lambda(2)$ can produce even stronger resonances in the mixed wave. In addition, it is significant that, while all three spectra in Fig. 3 show similar structure, the positions of the resonance peaks in Figs. 3(b) and 3(c) are shifted in $\lambda(2)$ relative to the corresponding peaks in Fig. 3(a) by an amount $\Delta\lambda$ which has the same sign as the corresponding detuning in $\lambda(1)$. For example, the values of $\lambda(1)$ and $\lambda(2)$ associated with the resonance peaks in Fig. 3(b) are both shifted by negative amounts relative to the values of $\lambda(1)$ and $\lambda(2)$ associated with the corresponding resonance peaks in Fig. 3(a). It results that a succession of resonance peaks in the mixed-wave signal can be obtained by a sequence of detunings of $\lambda(1)$ and $\lambda(2)$ of the same sign. But this allows the frequency $2\omega_1+\omega_2$ of the mixed-wave signal to be tuned over an appreciable range, corresponding to ranges of approximately 8 Å in $\lambda(1)$ and 11 Å in $\lambda(2)$. The effect observed here cannot be explained by the standard theory of the interaction based on perturbation theory.

Figure 4 shows the spectrum of the mixed-wave signal as a function of $\lambda(1)$ in the interval between 5600 and 5900 Å with the wavelength $\lambda(2)$ fixed at a value (5824

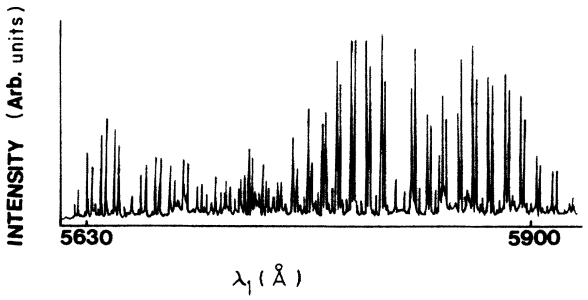

FIG. 4. Observed spectrum of mixed-wave signal as a function of the wavelength $\lambda(1)$ of beam 1 with the wavelength $\lambda(2)$ fixed at a value (5824 Å) lying close to a dominant resonance peak in Fig. 3.

Å) lying close to a dominant resonance peak in Fig. 3. The spectrum can in this case be interpreted to exhibit the structure of the second excited state of the molecule. The dominant features of the spectrum are produced by pairs of resonance peaks separated by approximately 9 Å. The mechanism which produces either the resonance pairs here or the similar doublet resonances in Fig. 3 is not yet understood. Spectra similar to that of Fig. 4 are obtained, however, from experiments in which $\lambda(2)$ is fixed at any wavelength in the range studied in Fig. 3. These spectra, along with the spectra of Fig. 3, can be used to study the properties of the excited states of I_2 molecules, but we choose here to emphasize only the implication of the spectra with respect to the tunability of the uv mixed-wave signal. From Figs. (3) and (4) one can see that, in principle, the simultaneous adjustment of the input wavelengths $\lambda(1)$ and $\lambda(2)$ allows this uv signal to be tuned over a range of hundreds of Å. Moreover, in contrast to the case of techniques in which tunability of the output signal is achieved by broadening the response (low Q), the tunability obtained here by shifting the resonant frequency of one beam via variation of the wavelength and power of a second beam is achieved with sharp resonances in $\lambda(1)$ and $\lambda(2)$.

In Fig. 5 we focus on a limited set of the resonance peaks in the mixed-wave spectra of Figs. 3 and 4 and emphasize certain characteristics of the data. In Fig. 5(a) the intensity of the mixed-wave signal at the two resonance peaks indicated by "1" and "2" in Fig. 3 is plotted as a function of the wavelength $\lambda(1)$ of beam 1. For a range of $\lambda(1)$ values in the vicinity of 5629.2 Å, a maximum intensity appears to occur periodically with a period in $\lambda(1)$ of approximately 0.4 Å. This periodicity is probably caused by the fact that variation of $\lambda(1)$ causes the energy of laser beam 1 to be brought successively into a simultaneous near coincidence with the energy differences corresponding to the $|0\rangle$-$|1\rangle$ and $|1\rangle$-$|2\rangle$ transitions in molecules with different values of the angular momentum quantum number J. For example, the intensity maximum in the narrow interval of $\lambda(1)$ values between 5629 and 5629.4 Å can be interpreted on the basis of the transition energy versus J diagram of Ref. 13 to be the result of a simultaneous nearresonance in the $|0\rangle$-$|1\rangle$ and $|1\rangle$-$|2\rangle$ transitions in molecules with quantum number $J=56$. We then interpret

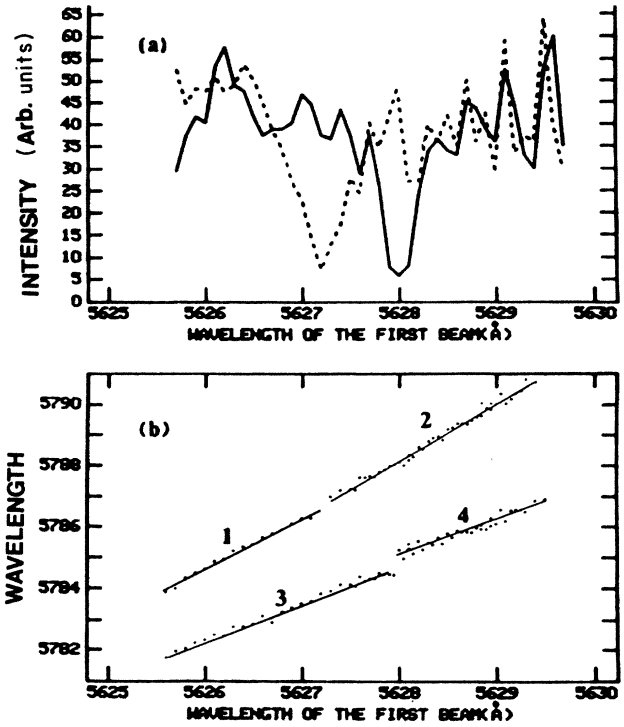

FIG. 5. (a) Intensity of the mixed-wave signal at the two resonance peaks indicated by "1" and "2" in Fig. 3, plotted as a function of the wavelength $\lambda(1)$ of beam 1 (dotted and solid lines corresponding to peaks 1 and 2, respectively). (b) Value of $\lambda(2)$ at a maximum in the mixed-wave signal plotted vs the corresponding value of $\lambda(1)$. Graphs 1 and 2 correspond to the left-hand peaks labeled by "1" in the pairs of resonance peaks in Fig. 3 while graphs 3 and 4 correspond to the right-hand peaks labeled by "2" in the same pair of peaks. Discontinuities appear to occur between the graphs 1 and 2 and between the graphs 3 and 4 at $\lambda(1)$ values which coincide with a relative minimum in the mixed-wave signal.

the variation in the maximum values of the different intensity peaks, and in particular the largest maximum in Fig. 5(a), to be the result of the interfering and mixing of the Stark-shifted energy levels of the total molecule-field system when two or three of these levels are tuned close to each other.

Because two laser beams are required to produce the mixed-wave output signal, the relationship between the wavelengths of the two beams at the resonance peak is interesting. Figure 5(b) shows graphs of the value of $\lambda(2)$ at a maximum in the mixed-wave signal versus the corresponding value of $\lambda(1)$ (with the power of beam 1 approximately 0.7 mJ/pulse). Graphs 1 and 2 correspond to the first (left-hand) peaks in the pairs of resonance peaks in Figs. 3 and 4, while graphs 3 and 4 correspond to the second (right-hand) peaks in the same figures. The slopes of the four graphs are probably connected to the rotational constants B of the excited molecules.[13] The graphs of Fig. 5(b) suggest that discontinuities occur in the relationships between the resonance values of $\lambda(1)$ and $\lambda(2)$ which correspond to the first and second resonance peaks at $\lambda(1)$ values of 5627.2 and

5628 Å, respectively. A comparison of Figs. 5(a) and 5(b) shows that these discontinuities coincide with minimum values for the heights of the corresponding resonance peaks. The connection between Figs. 5(a) and 5(b) is not yet fully understood, but the discontinuous slope changes in the graphs of Fig. 5(b) suggest that the resonant wave-mixing process corresponding to different intervals of $\lambda(1)$ and $\lambda(2)$ involves two distinct sets of vibronic-rotational states associated with distinct rotational constants.

The scattering of the experimental points about the straight lines in Fig. 5(b) is not entirely the result of random noise in the data. In Fig. 6 we graph on an enlarged scale part of the same data shown in Fig. 5 which relates to the second (or right-hand) peak in the sets of paired resonances in Figs. 3 and 4. Figure 6(a) shows detailed features, of the solid graph of Fig. 5(a) in the region of $\lambda(1)$ values between 5628.3 and 5630 Å, while Fig. 6(b) shows details of graph 4 in Fig. 5 (b) in the same region. The graph, Fig. 6(c), shows data similar to that shown in the graph, Fig. 6(b), for the case that the input intensity of beam 1 is increased to 2.0 mJ/pulse. It can be seen from the graphs, Figs. 6(b) and 6(c), that while the value of $\lambda(2)$ corresponding to a mixed-wave maximum consistently increases with increasing $\lambda(1)$ on a large scale of variations, it can decrease with increasing $\lambda(1)$ on a smaller scale of variations, the latter effect being enhanced at higher input intensity for beam 1. In addition it can be seen from the graphs, Figs. 6(a), (6b), and 6(c), that the relationship between the resonant $\lambda(1)$ and $\lambda(2)$ values appears to exhibit a discontinuity at the $\lambda(1)$ values that are close to the values for which a local maximum in the output intensity occurs. Moreover, because the discontinuity appears to increase with the input power of beam 1 it can be assumed to be a consequence of the ac Stark effect.

The origin of this discontinuity in the uv output intensity can be easily understood on the basis of the discussion given in the last paragraph of Sec. II. The value of $\lambda(1)$ determines the values of the two detunings Δ_1 and Δ_2 and therefore the value of Δ_2-Δ_1, while the value of $\lambda(2)$ determines the overall detuning δ and approximately fixes the position of the dressed level 3′. As discussed in Sec. II, a change in the sign of Δ_2-Δ_1 produces an interchange in the dressed levels 1′ and 2′ and a resultant large shift in the positions of these two levels. Therefore, if the dominant resonance in the output signal as a function of $\lambda(2)$ occurs when the dressed level 3′ crosses or anticrosses with one of the dressed levels 1′ or 2′, a small change in the value of $\lambda(1)$ in the vicinity of the $\lambda(1)$ value for which $\Delta_1=\Delta_2$ can change the sign of $\Delta_2-\Delta_1$ and thus require a large change in the value of $\lambda(2)$ to keep level 3′ in coincidence with either level 1′ or 2′. It is this effect that is expected to account for the discontinuous relation between the resonance values of $\lambda(1)$ and $\lambda(2)$ observed in Fig. 6 when the intensity of the mixed-wave resonance has its maximum value.

A more quantitative comparison between the experimental results shown in Fig. 6 and the theoretical model developed here is shown in Fig. 7. The solid and dashed theoretical curves in this figure are calculated by determining the $\lambda(1)$ and $\lambda(2)$ values corresponding to the condition under which we expect a dominant mixed-wave resonance to occur, this condition being that $\delta=\lambda_1$ or λ_2. For a chosen value of $\lambda(1)$ we compute the corre-

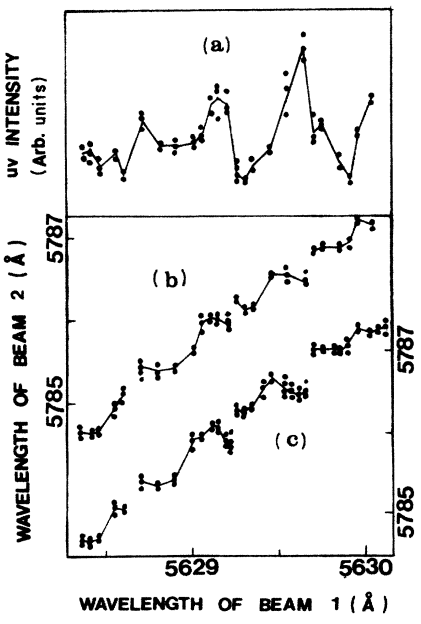

FIG. 6. (a) Detailed features of the solid graph shown in Fig. 5(a) for $\lambda(1)$ values in the interval between 5628.3 and 5630 Å. (b) Detailed features of graph 4 in Fig. 5(b) with the input power of beam 1 equal to that corresponding to Fig. 5, 0.7 mJ/pulse. (c) Data similar to that shown in (b) for the case that the input power of beam 1 is increased to 2.0 mJ/pulse. The scale for (c) is on the right-hand side of the diagram.

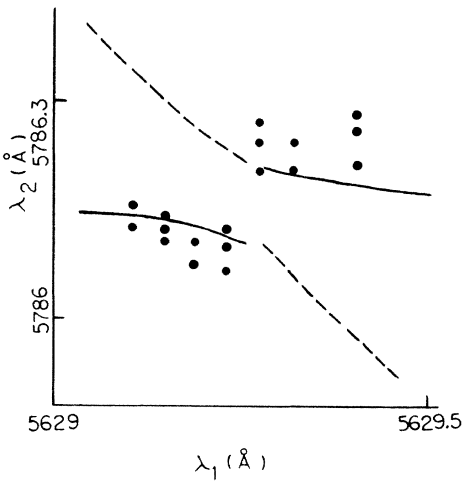

FIG. 7. Graph similar to plots shown in Figs. 5(b) and 6(b), showing comparison between theory and experiment. Dots represent experimental data points. Solid and dashed lines represent values of $\lambda(2)$ vs $\lambda(1)$ at a maximum in the mixed-wave signal calculated by setting the detuning in state 3, δ equal to the eigenvalue of dressed level $|2'\rangle$ (λ_2 in the text), and $|1'\rangle$ (λ_1 in the text), respectively.

sponding eigenvalues of levels $|0'\rangle$, $|1'\rangle$, and $|2'\rangle$ by solving the eigenvalue equation (Eq. 15) with $a=2.0$ GHz, $b=7.0$ GHz, and $c=0$ (i.e., we diagonalize a 3×3 matrix under this condition) and the value of $\lambda(2)$ is then determined by setting $\delta=\lambda_1$ or λ_2. The energy of levels 0 and 1 is calculated from the formula given by Wei and Tellinghuisen[20] while that of level 2 is calculated from the wavelength of beam 1, $\lambda(1)$, with the assumption that the double resonance under the condition $\Delta_1=\Delta_2$ gives maximum intensity in the resonant uv output. The chosen value of $\lambda(1)$ thus fixes the value of Δ_1 and Δ_2. The solid curve, corresponding to the condition $\delta=\lambda_2$, is in reasonable agreement with the data representing repeated measurements shown as dots in this diagram. In particular, the discontinuity in the solid curve is consistent with the observed discontinuity in the relationship between the resonance values of $\lambda(1)$ and $\lambda(2)$. We conclude from the comparison that the dominant resonance in the mixed-wave signal results from the anticrossing of the dressed levels 3′ and 2′ (rather than from the anticrossing of levels 3′ and 1′). It is significant that the values for the constants a and b used in the above calculation agree reasonably well with the values for a and b estimated from a previous experimental investigation.[14]

IV. CONCLUSION

A resonant enhancement is observed in the wave-mixing signal derived from a four-level system when neither the one-, two-, nor three-quantum transition in the free molecule is in resonance with the exciting light. The resonant enhancement is believed to arise due to the ac Stark effect which, for certain detunings of the incident light beams, allows the dressed levels of the total molecule-field system to "anticross" and thereby produce a resonance in the mixed-wave intensity. A large amount of data is presented to show that by continuous tuning of the frequencies of the incident beams a relatively large mixed-wave signal can be obtained with mixed-wave wavelengths in a range of hundreds of angstroms. A simple nonperturbative semiclassical theory is made use of to explain certain interesting features of the data. In particular, the discontinuity observed in the relationship between the resonance values of the laser beam wavelengths can be interpreted in terms of the ac Stark shift of the dressed levels of the molecule-field system. In addition, an observed periodic variation in the amplitude of the mixed-wave resonance as a function of the wavelength of the high intensity input laser may be consistent with the prediction of the theory that the mixed-wave resonance becomes a maximum when the eigenenergies of three dressed levels, λ_1, λ_2, and λ_3, are tuned close to each other. Because we show that the output intensity at the mixed-wave frequency is continuously tunable over a wide range of frequencies, the technique described here may be valuable in providing a source of continuously tunable light in the ultraviolet and vacuum-ultraviolet regions of the spectrum.

On the other hand, the semiclassical theory developed in this work may be too simple to explain some of the experimental results. In particular, the homogeneous and inhomogeneous linewidths, which are discussed only qualitatively in connection with the limitations they impose on the applicability of the formula for the time evolution of the density matrix, should play an important role in determining the line shape of the resonances. However, the usual theory of the molecule-field interaction based on the optical Bloch equations or on strict rate equations is too complicated in the physical case considered to allow for a physical picture of the process which produces the observed resonances, and these resonances are not predicted by the theory based on perturbation techniques. Nevertheless, an alternative theory to that developed here,[21] which is based on simplified Bloch equations that treat the transition between molecular levels $|0\rangle$ and $|2\rangle$ as a one-step process, also predicts the dominant resonance which is found in this work.

The spectra observed in the experimental work which we report on may also be valuable for the study of excited states in molecules. Since there has been extensive theoretical work on the energy levels of halide molecules, especially I_2, a comparison of the theoretical predictions with the spectra obtained here may also be interesting.

[1] A. M. Bonch-Bruevich and V. A. Khodovoi, Usp. Fiz. Nauk **93**, 71 (1967) [Sov. Phys.—Usp. **10**, 637 (1968)].

[2] S. H. Autler and C. H. Townes, Phys. Rev. **100**, 703 (1955).

[3] C. Cohen-Tannoudji, Metrologia **13**, 161 (1977).

[4] B. R. Mollow, Phys. Rev. **188**, 1969 (1969).

[5] F. Schuda, C. R. Stroud, Jr., and M. Hercher, J. Phys. B **7**, L198 (1974); J. Morellec, D. Normand, and G. Petite, Phys. Rev. A **14**, 300 (1976).

[6] P. Kruit, W. R. Garrett, J. Kimman, and M. J. Van der Wiel, J. Phys. B **16**, 3191 (1984); M. S. Pindzola and A. H. Glasser, Phys. Rev. A **30**, 1800 (1984).

[7] J. L. Picque and J. Pinard, J. Phys. B **9**, L77 (1976); J. E. Bjorkholm and P. F. Liao, Opt. Commun. **21**, 132 (1977); H. R. Gray and C. R. Stroud, *ibid.* **25**, 359 (1978).

[8] A. Schabert, R. Keil, and P. E. Toschek, Appl. Phys. **6**, 181 (1975); Ph. Cahuzac and R. Vetter, Phys. Rev. A **14**, 270 (1976); C. Delsart and J.-C. Keller, J. Phys. B **13**, 241 (1980); J. Phys. (Paris) **42**, 529 (1981).

[9] F. Y. Wu, R. E. Grove, and S. Ezekiel, Phys. Rev. Lett. **35**, 1426 (1975); Phys. Rev. A **15**, 227 (1977); W. Hartig, W. Rasmussen, R. Schieder, and H. Walther, Z. Phys. A **278**, 205 (1976).

[10] M. Arditi and J.-L. Picque, J. Phys. B **8**, L331 (1975); P. F. Liao and J. E. Bjorkholm, Phys. Rev. Lett. **34**, 1 (1975); Opt. Commun. **16**, 392 (1976); S. Reynaud, M. Himbert, J. Dupont-Roc, H. H. Stroke, and C. Cohen-Tannoudji, Phys. Rev. Lett. **42**, 756 (1979).

[11] F. Y. Wu, S. Ezekiel, M. Ducloy, and B. R. Mollow, Phys.

Rev. Lett. **38**, 1077 (1977); D. J. Harter and R. W. Boyd, IEEE J. Quantum Electron. **QE-16**, 1126 (1980); D. J. Harter, P. Narum, M. G. Raymer, and R. W. Boyd, Phys. Rev. Lett. **46**, 1192 (1981); D. J. Harter and R. W. Boyd, Phys. Rev. A **29**, 739 (1984).

[12]P. D. Kleiber, K. Burnett, and J. Cooper, Phys. Rev. A **25**, 1188 (1982).

[13]C. Tai, C. C. Kim, R. T. Deck, and Y. Wu, Phys. Rev. A **33**, 3970 (1986).

[14]C. Tai and Y. Wu, Opt. Commun. **58**, 217 (1986).

[15]C. Tai, F. W. Dalby, and G. L. Giles, Phys. Rev. A **20**, 233 (1979).

[16]C. Cohen-Tannoudji and S. Reynaud, J. Phys. B **10**, 345 (1977); E. Coutens and A. Szoke, Phys. Rev. A **15**, 1588 (1977).

[17]For example, Y. R. Shen, *The Principles of Nonlinear Optics* (Wiley, New York, 1984).

[18]R. M. Whitley and C. R. Stroud, Jr., Phys. Rev. A **14**, 1498 (1976).

[19]J. H. Eberly, B. W. Shore, Z. Bialynicka-Birula, and I. Bialynicka-Birula, Phys. Rev. A **16**, 2038 (1977).

[20]J. Wei and J. Tellinghuisen, J. Mol. Spectrosc. **50**, 317 (1974).

[21]Pin Fan Tang, Masters thesis, University of Toledo, 1986.